CIVIL ENGINEERING JOURNAL

Article no. 4

THE CIVIL ENGINEERING JOURNAL 1-2026

REGARDING SEVERAL NEW CRITERIA FOR THE ENERGY-EFFICIENT ENVELOPE'S POTENTIAL ASSESSMENT

Yuriy Biks[1], Georgiy Ratushnyak[2] and Olga Ratushnyak[3]

1. *Vinnytsia National Technical University, Faculty of Construction, Civil and Environmental Engineering, Department of Construction, Architecture and Urban Planning, Vinnytsia, Politekhnichna 7, Ukraine; biks@vntu.edu.ua*
2. *Vinnytsia National Technical University, Faculty of Construction, Civil and Environmental Engineering, Department of Engineering Systems in Construction, Vinnytsia, Politekhnichna 7, Ukraine; ratushnyak@vntu.edu.ua*
3. *Vinnytsia National Technical University, Faculty of Management and Information Security, Department of Business Economics and Production Management, Vinnytsia, Khmelnytske Highway 95, Ukraine; ratushniak@vntu.edu.ua*

Received: *28.05.2025*

Received in revised form: *21.01.2026*

Accepted: *19.03.2026*

ABSTRACT

This paper introduces a set of new criteria for assessing the energy-efficiency potential of multilayered building envelopes, focusing on physically measurable aspects of dynamic thermal performance and LCA parameters. Based on EN ISO 13786:2023, the study considers thermal transmittance (U-value), internal areal heat capacity (k_1), and decrement factor (f) as thermal performance parameters, along with assembly mass (m) and embodied energy (EE) as additional LCA objective indicators. Five wall assemblies common in the Ukrainian market - hempcrete, AAC + Rockwool, Porotherm brickwork + Rockwool, wood-chip cement-bonded blocks (Woodcrete) and ICF systems were evaluated through numerical modelling and comparative analysis. To eliminate subjectivity in criteria weighting, three new interconnected criteria were proposed: Dynamic Thermal Performance Efficiency per mass ($DTPE_m$), per embodied energy ($DTPE_{EE}$), and per both ($DTPE_{m\&EE}$). Results indicate that AAC + Rockwool (Wall B) consistently ranks as the most efficient assembly according to the $DTPE_{m\&EE}$ criteria. At the same time, Wall E (ICF) aligns with the recommended thermal inertia ranges but exhibits the highest embodied energy, resulting in the lowest $DTPE_{m\&EE}$. The study highlights the complexity of MCDA in envelope design and provides physically grounded criteria that can support more objective predesign decision-making.

KEYWORDS

Dynamic thermal performance efficiency, Multilayered assembly, Envelopes, Energy efficiency, Physical parameters

INTRODUCTION

The diverse range of building materials and construction techniques in modern practice has drawn significant attention from multicriteria decision analysis (MCDA) methods [1], particularly for

determining building energy efficiency, as evidenced in papers [1], [2], [3], [4]. From a practical perspective, such research aims to identify criteria for energy efficiency that are both interpretable and adjustable [5]. Such criteria are results of complex interconnection of thermal and physical behaviour parameters of the multilayered envelope itself (e.g. U-value [5], [6], [7] thermal inertia [4], [8], [9], internal area heat capacity [5], [10] decrement factor [5], [9]), climate influence (e.g. hot degree days HDD, cool degree days CDD), building orientation towards the sun (e.g. Trombe wall in the south façade, opaque north-oriented wall [11]), etc. All of the studies mentioned above demonstrate that efforts to establish comprehensive criteria for evaluating envelope energy efficiency remain relevant [8]. Meanwhile, one of the major, if not the most crucial, ongoing predesign stage challenges for developers is selecting the "best" option from the vast array of available building envelopes. However, comparisons between alternatives typically involve trade-offs, making the selection of the optimal or "best" solution inherently complex. The term "best" is used here with caution, as a multicriteria assessment of real-life alternatives often suggests that only options within the Pareto set can be deemed the "best" or optimal alternatives [2], [3], [4], [5], [12], [13]. In practice, new criteria could allow the decision-maker to pick the better Pareto-set solution that dominates others by this additional criterion, and provides the most advantageous overall compromise [13].

To facilitate the decision-making process during the early stages of building design, easily calculable physical criteria were chosen, including thermal transmittance (U-value), W/m²K, mass (m, kg/m²), decrement factor (f) and internal area heat capacity (k_1), kJ/m²K, based on dynamic thermal performance standards outlined in Ukraine National Standard DSTU EN ISO 13786 [6] and embodied energy or primary energy of the wall component MJ/m², as the objective LCA marker [14], [15].

LITERARY ANALYSIS AND PROBLEM STATEMENT

In recent decades, the performance assessment of building envelopes has shifted gradually from simple one-dimensional thermal resistance comparisons to integrative frameworks that include dynamic, environmental, and lifecycle-aware indicators [2], [4], [7], [8]. Traditionally, steady-state criteria, such as the thermal transmittance coefficient (U-value), have served as the primary determinant of envelope efficiency. However, as numerous authors have pointed out [8], [15], [16], [17], this parameter alone fails to accurately reflect the dynamic thermal behaviour of constructions and their inertia-related performance, especially under real-time climatic fluctuations [15], [16]. In climates with sharp day-night cycles or seasonally variable thermal loads, parameters such as thermal mass, decrement factor, and phase shift have emerged as crucial in describing a wall's ability to modulate indoor comfort and energy demand [15], [17].

At the same time, material-related physical and mechanical properties, including density, specific heat capacity, and moisture behaviour, influence not only dynamic heat flow but also structural performance and lifecycle impacts. This intersection of thermal behaviour and material ecology has prompted scholars to develop composite indicators aligned with Life Cycle Assessment (LCA) methodologies [5], [18], [19]. Several studies suggest that the embodied energy of materials, coupled with their service life, should be internalised in envelope selection, particularly when aiming to balance operational and embodied performance [15].

However, a comparative deficiency remains in the literature regarding integral metrics that connect physical, mechanical, and lifecycle properties as an actionable selection tool for design optimisation. While LCA tools provide environmental insights, U-value (W/m²K), internal area heat capacity (k_1), kJ/m²K, and the decrement factor (f) reflect thermal parameters that are primary influencers of envelope winter and summer behaviour [8], there is limited methodological convergence between them. Some attempts to bridge this include thermal mass assessments [20], [21] or dynamic-to-static performance coefficients [15]; however, such indicators have yet to be standardised or validated across material groups.

Thus, the current research aims to critically explore new criteria, grounded in physical and mechanical properties, such as internal area heat capacity and decrement factor, as dynamic thermal inertia indices, in conjunction with environmental durability parameters, including Life Cycle Assessment (LCA).

PURPOSE AND TASKS OF RESEARCH

The current research aims to formulate additional criteria for early-stage multilayered assembly design assessment of envelope energy-efficiency potential, based exclusively on physical parameters of envelope materials and taking into account dynamic thermal characteristics as well as embodied energy as the LCA component, which can provide a more objective comparison of different envelope types in terms of their thermophysical and physical-mechanical parameters. This direction is particularly relevant given the rising need for buildings that harmonise material rationality, climate adaptability, and lifecycle sustainability.

To achieve this goal, the following tasks should be solved:

a) a list of envelope types for the medium cost segment of residential buildings, based on the conducted data review, should be revealed.

b) the most significant physical and thermophysical parameters for the complex multi-criteria should be chosen;

c) a complex multi-criteria parameter should be proposed, and the benchmarking of the proposed envelope types should be calculated.

MATERIALS AND METHODS

The physical criteria that could easily be calculated in the early-stage multi-layered assembly design of the construction, such as thermal transmittance (U-value), W/m^{2}K, mass (m, kg/m^2), and internal area heat capacity (k_1), kJ/m^{2}K, as a dynamic thermal performance parameter under EN ISO 13786 [1] for the wall assembly, were taken.

For the calculation of the EE (research LCA framework is limited to the material production stages A1-A3 values only), the MJ/m² of relevant assembly materials was mainly determined using the Baubook Eco2soft online tool [22] and data from the research papers.

The numerical assessment of dynamic thermal performance efficiency parameters, such as thermal transmittance (U-value), W/m²K, the decrement factor (f), and internal area heat capacity (k1), kJ/m²K, was performed using the HTflux [23] freely downloadable Excel-based calculator spreadsheets.

For numerical simulation setup of the dynamic thermal performance efficiency parameters, as well of EE parameter, five types of multilayered wall assemblies, were chosen as popular assemblies in the Ukrainian construction market, namely: Wall A (Hempcrete) as energy efficient and eco-friendly type, Wall B (Aerated autoclaved concrete (AAC) D300 + Rockwool as insulation material) as the affordable cost-efficient type of energy efficient solution; Wall C (Hollow brickwork masonry (Porotherm 38) + Rockwool as insulation material) as traditional reliable ceramic brickwork masonry with energy efficient porous brick, Wall D (Wood-chip cement bonded block) as energy efficient and “retrofitted” technology and Wall E (wood-chip cement bonded block, as one of the promising type of Insulated concrete formwork (ICF), which gained a significant traction in EU, North American and Australian construction market and is commercially distributed under trademarks as ISOTEX [24], [25], Fixolite [26], Isolabloc [27], Isospan [28], Fasswall [29], Nexcem [30], Durisol [31] etc.) as well-known wall construction technology in European, North American and Australian construction markets and new construction technology competitor at the Ukrainian one. In Figures 1-5, there are photos from real construction sites showing the investigated assemblies, and in Figure 6, a detailed cross-section drawing.

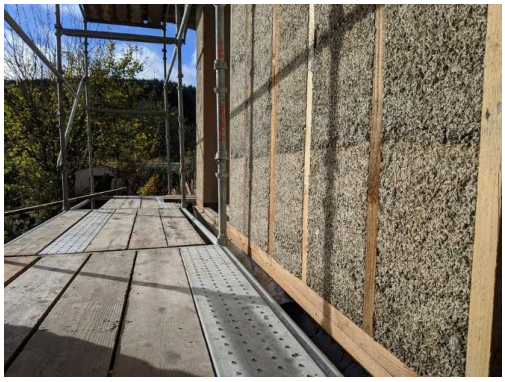

Fig. 1 – Hempcrete wall performed by tamping method (Photo taken from [32])

Fig. 2 – AAC façade insulated with stone-wool wall insulator (Photo taken from [33])

Fig. 3 – Layering of hollow ceramic blocks (Porotherm 38, Photo taken from [34])

Fig. 4 – Layering of wood-chip cement-bonded blocks (Photo taken from [35][34])

Fig. 5 – Layering of ISOTEX - ICF wood-chip cement-bonded blocks (Photo taken from [36][35][34])

The dynamic thermal characteristics of each multilayered assembly were determined below under ISO 13786 [6] using the following sequence:

1) Definition of thermophysical properties (ρ, c, λ) for each layer (see Tab.1);
2) Calculation of penetration depth;
3) Determination of dimensionless thickness;
4) Construction of layer transfer matrices;
5) Assembly of the global transmittance matrix;
6) Extraction of dynamic parameters: internal areal heat capacity (k_1), decrement factor (f).

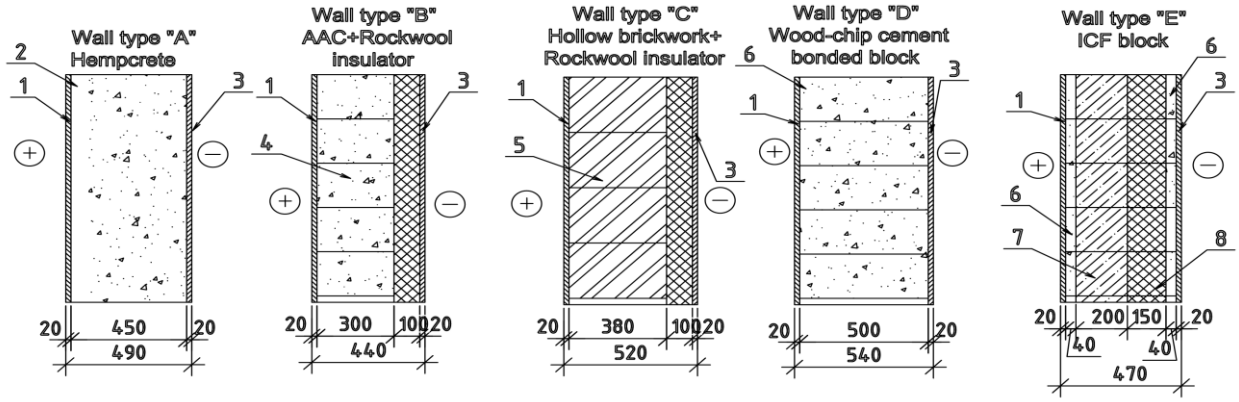

Fig. 6 – Cross-sectional scheme of investigated wall assemblies: (1 - internal lime-sand plaster, 2 - hemcrete, 3 - external lime-sand plaster, 4 - aerated autoclaved concrete (AAC), 5 - hollow brick-work, 6 - wood-chip cement bonded block (woodcrete), 7 - reinforced concrete, 8 - BASF Neopor insulator)

The calculations were implemented in a spreadsheet environment [23] and verified through consistency checks and comparison with literature values (given below).

Thermal transmittance (U-value) under [37] of the aforementioned multilayered assemblies is calculated as follows in Equation (1)

$$\mathrm{U-value} = \frac{1}{R_{si}+\sum_{i=1}^{n}\frac{d_i}{\lambda_i}+R_{se}}, \quad (1)$$

where R_{si}=1/8.7- interior layer thermal resistance, m^{2}K/W [38];
R_{se}=1/23 – exterior layer thermal resistance, m^{2}K/W [38];

d_i, λ_i – the thickness and thermal conductivity coefficient of the *i*-th layer, respectively.

Penetration depth of the *i*-th layer under [6] is calculated according to the formula (2)

$$\delta_i = \sqrt{\frac{\lambda_i \times T}{\pi \times \rho_i \times c_i}}, \quad (2)$$

where T=24hours – oscillation time, considered for envelopes;

ρ_i, c_i – the density and specific heat capacity of the *i*-th layer.

Dimensionless penetration depth under [6] is calculated as represented in the formula (3)

$$\xi = \frac{d_i}{\delta_i}. \quad (3)$$

Thermal transmittance matrix component of each i-th layer under [6] is calculated as follows in formulae (4)-(6)

$$z11_i = z22_i = \cos(\xi_i \times (1i - 1)), \quad (4)$$

where $1i = \sqrt{-1}$.

$$z12i = -\frac{\delta_i}{2 \times \lambda_i} \times (-1i - 1) \times \sin(\xi_i \times 1i - \xi_i); \quad (5)$$

$$z21i = -\frac{\lambda_i}{\delta_i} \times (-1i - 1) \times \sin(\xi_i \times 1i - \xi_i). \quad (6)$$

Thus, the transmittance matrix of the i-th layer is defined as [6] and is to be arranged as in formula (7)

$$Z_i = \begin{bmatrix} z11_i & z12_i \\ z21_i & z22_i \end{bmatrix}. \quad (7)$$

In case we have a multilayered envelope, the total transmittance matrix will be the product of the total transmittance matrix Z_{tot} of each *i*-th layer, from the interior to exterior, in terms of envelope cross-section, as it is represented in formula (8)

$$Z_{tot} = \prod_{i=1}^{k} Z_i, \quad (8)$$

where $k = 1,2,\dots,n$ – number of layers.

The boundary layer thermal transmittance matrix under [6] is calculated as follows in formula (9)

$$Z_{s1} = \begin{bmatrix} 1 & -R_{se} \\ 0 & 1 \end{bmatrix}; \quad (9)$$

$$Z_{s2} = \begin{bmatrix} 1 & -R_{si} \\ 0 & 1 \end{bmatrix}. \quad (10)$$

Construction thermal transmittance matrix of multilayered envelope from environment to environment, according to [6], to be calculated as defined in formula (11)

$$Z_{ee} = Z_{s2} \times Z_{tot} \times Z_{s1} \quad (11)$$

Internal area heat capacity (k_1) and decrement factor (f) under [6] are to be calculated as defined in formulae (12)-(13)

$$k_1 = \left| \frac{Z_{ee_{2,2}}{}^{-1}}{Z_{ee_{1,2}}} \right| \times \frac{T}{2 \times \pi}; \quad (12)$$

$$f = \frac{\left| \frac{Z_{ee_{2,2}}{}^{-1}}{Z_{ee_{1,2}}} \right| \times \frac{T}{2 \times \pi}}{U\text{-}value}, \quad (13)$$

where $Z_{ee2,2}$, $Z_{ee1,2}$–elements of the second column of the second row and the second column of the first row of the construction thermal transmittance matrix, respectively.

The initial thermophysical parameters of the assembly materials used in the current numerical experiment (numerator), obtained from the referenced data range (denominator), are aggregated in Table 1.

Tab. 1 - The initial thermophysical parameters of assembly materials

Assembly material	The thermophysical parameters of materials			Data reference
	Specific heat capacity, *c* (J/kgK)	Density ρ, (kg/m³)	Thermal conductivity λ, (W/m·K)	
Lime-sand plaster	1000	1500	0.67	[39][39]
Hempcrete	$\frac{1200}{1000-1600}$	$\frac{450}{200-627}$	$\frac{0.08}{0.05-0.18}$	[40], [41], [42], [43], [44]
Aerated autoclaved concrete (AAC)	100	275	0.09	[39]
Hollow brickwork masonry (Porotherm 38 W)	1000	745	0.112	[39], [45], [46]
Wood-chip cement-bonded block	$\frac{1400}{1000-1700}$	$\frac{475}{475-587}$	$\frac{0.12}{0.1-0.12}$	[24], [25], [26], [27], [28], [29], [30], [31]
Reinforced concrete	1000	2200	1.65	[22], [39]
BASF Neopor insulator	$\frac{1450}{1200-1600}$	$\frac{16}{15-25}$	$\frac{0.031}{0.031-0.032}$	[39][22], [39], [47]
Stone wool wall insulator (Rockwool®)	$\frac{1030}{800-1030}$	$\frac{70}{30-200}$	$\frac{0.034}{0.033-0.045}$	[39]

For the calculation of the EE (research focuses only on the material production stages A1-A3 values of the LCA framework), the MJ/m² of each assembly was determined using the Baubook Eco2soft online tool [22]. The output influence parameters for all the assemblies are calculated in Table 2.

Tab. 2 - Calculated parameters for researched assemblies

Influence parameter	Wall type "A"	Wall type "B"	Wall type "C"	Wall type "D"	Wall type "E"
U-value, W/m²K	0.17*	0.15	0.15	0.22	0.17
m, kg/m²	262.50	149.50	350.10	335.00	540.39
k_1, kJ/m²K	39.955	37.369	43.742	43.551	40.073
f	0.013	0.115	0.007	0.007	0.052
EE, MJ/m²	833.55**	594	951	889	770

*For simplicity, the timber frame input is not taken into consideration;

**For Wall A, the *EE* value was calculated as:

$$3.5 \cdot 0.45 \cdot 450 + 2.08 \cdot 2 \cdot 0.02 \cdot 1500 = 833.55 \frac{MJ}{m^2},$$

where 3.5 – *EE* of hemp-lime composite, MJ/kg, taken from [44];

2.08 – *EE* for one-layer plastering mortar for external OC lime (1500 kg/m³), MJ/kg, taken from Eco2soft database [22][22];

0.45, 0.02 – hempcrete wall and external and internal plaster thicknesses, respectively, m;

450, 1500 – densities of the hempcrete wall and plaster, respectively, kg/m³ (see Table 1).

From the analysis of Table 2, it can be seen that all the researched assemblies meet the minimum permissible reduced heat transfer resistance for enclosing structures of residential and public buildings, as required in Ukraine. $R_{qmin} = 4.0\ \frac{m^2\mathrm{K}}{\mathrm{W}}$ [49][49], or by a more convenient unit $\mathrm{U-value} = \frac{1}{R_{qmin}} = 0.25\ \frac{\mathrm{W}}{m^2\mathrm{K}}$ with significant energy efficiency potential (wall B and wall C, respectively, with the same $\mathrm{U-value} = 0.15 \frac{\mathrm{W}}{m^2\mathrm{K}}$. Wall A and Wall E also demonstrate a sufficient level of $\mathrm{U-value} = 0.17 \frac{\mathrm{W}}{m^2\mathrm{K}}$. The last preferable Wall type from the perspective of thermal transmittance is Wall D with $\mathrm{U-value} = 0.22 \frac{\mathrm{W}}{m^2\mathrm{K}}$.

To ensure the reliability of the results, the calculated dynamic parameters were compared with reference ranges reported in several relevant studies on the thermal inertia of building envelopes [8], [15], [16], [50], [51], [52] The values of the decrement factor and internal specific heat capacity fall within expected ranges for similar constructions, confirming the validity of the applied methodology.

From the dynamic performance characteristics, such as (k_1) and (f), together with the U-value, which are considered significant influencers of summer and winter behaviour [8], the overall picture of the preferred wall assembly becomes more complicated. The comparison of the (k_1) versus density shows that the massive wall assemblies will possess a higher value of internal area heat capacity (k_1), which is neither good nor bad. The higher (k_1) value should provide more comfortable interior temperatures on a hot summer day due to its greater heat-accumulation capacity.

Geographically, Vinnytsia city, a representative city of central Ukraine, was selected as an example city. The construction of the aforementioned assemblies was numerically modelled on a typical July day (to see the "true" picture without HVAC intervention) to provide a graphical representation of temperature and heat-flow attenuation, as an additional aspect of wall dynamic behaviour. The climate of the aforementioned city can be described as follows:

- Humid continental climate - warm summer, no dry season (climate zone Dfb by Köppen–Geiger Classification) [53]; Cold winters often below 0 °C, warm summers (average July ≈ 19 - 21 °C [53][54]), precipitation fairly evenly distributed year-round [55]; Climate is heating-dominated. Heating Degree Days for a typical year (HDD) = 3676 °C·days/year (base 20 °C, [55]); Indicates high heating demand during a long heating season (roughly October–April);
- Reflects low cooling demand, with only short periods of summer overheating. Cooling Degree Days (CDD) are not presented in the current version of Norm [55], but could be approximately evaluated for a typical year as $D \times (T_{av} - T_{base}) \approx 8 \times (23.5 - 22) \approx 12$ °C·days/year, where D – days through the year with average diurnal temperature T_{av} higher than the threshold T_{base} = 22°C;
- Thermal design focus: insulation, thermal mass, and minimising heat losses; Summer overheating is moderate, but it can matter for lightweight buildings. Input data for HTflux modelling [23] are presented in Table 3.

Tab. 3 - Initial data for dynamic simulation of the Wall A

Mean temperature side 1 (ext.):	25.5°C	Mean temperature side 2 (int.):	25.0°C
Temp. Amplitude side 1 (ext.):	9.0°C	Temp. Amplitude side 2 (int.):	1.5°C
Time of max. Temp side 1 (ext.):	15:00	Time of max. Temp side 2 (int.):	17:00

Figure 7 illustrates results from the dynamic heat-flow simulation on both the external and internal sides of each wall, including heat flow and temperature fluctuations, as output from the HTflux spreadsheet [23].

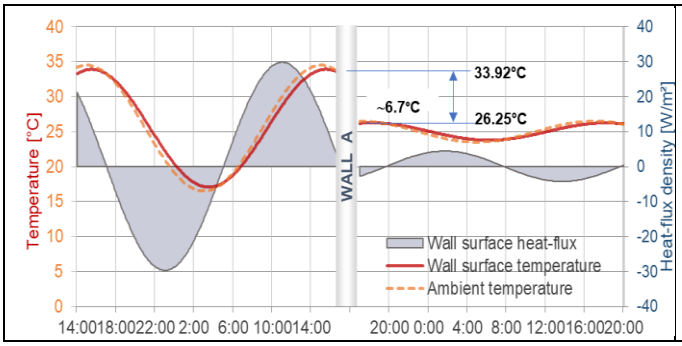

Building component surface temperature	
side 1	side 2
Max: 33.92°C	Max: 26.25 °C
Min: -17.08°C	Min: 23.77 °C
Range: 16.84°C	Range: 2.47 °C
Building component heat flux	
side 1	side 2
Max: 29.85W/m²	Max: 4.43 W/m²
Min: -29.68 W/m²	Min: -4.26 W/m²
Range: 59.52 W/m²	Range: 8.69 W/m²

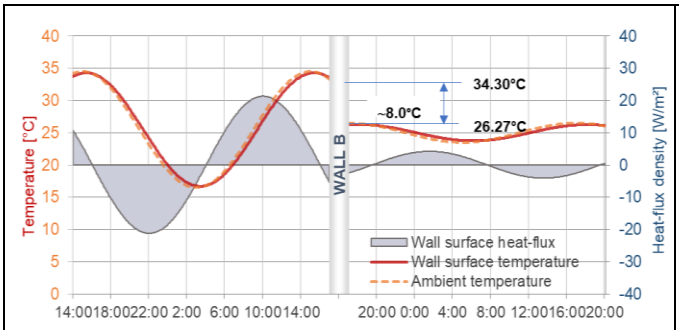

Building component surface temperature	
side 1	side 2
Max: 34.30 °C	Max: 26.27 °C
Min: -16.69 °C	Min: 23.75 °C
Range:17.60 °C	Range: 2.52 °C
Building component heat flux	
side 1	side 2
Max: 21.35 W/m²	Max: 4.23 W/m²
Min: -21.20 W/m²	Min: -4.07 W/m²
Range: 42.55 W/m²	Range: 8.30 W/m²

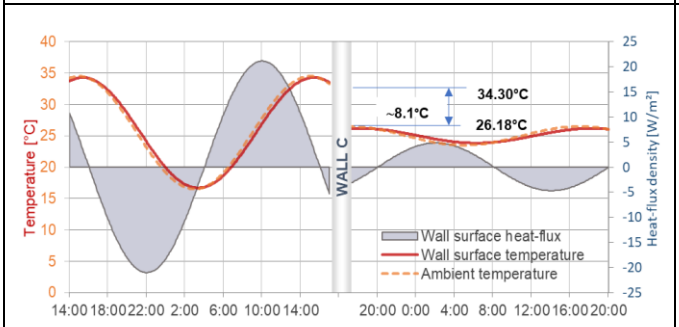

Building component surface temperature	
side 1	side 2
Max: 34.30 °C	Max: 26.18 °C
Min: -16.70 °C	Min: 23.84 °C
Range:17.60 °C	Range: 2.34 °C
Building component heat flux	
side 1	side 2
Max: 21.17 W/m²	Max: 4.84 W/m²
Min: -21.02 W/m²	Min: -4.69 W/m²
Range: 42.19 W/m²	Range: 9.53 W/m²

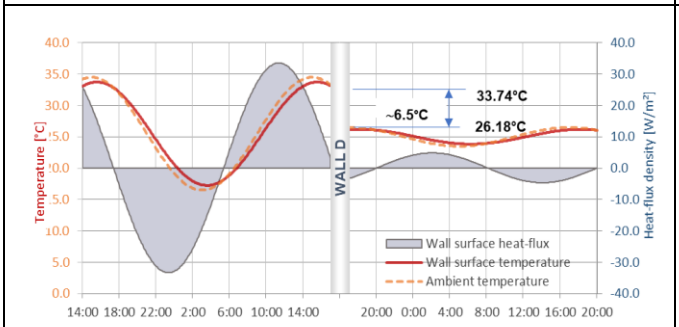

Building component surface temperature	
side 1	side 2
Max: 33.74 °C	Max: 26.18 °C
Min: -17.25 °C	Min: 23.84 °C
Range: 16.49 °C	Range: 2.34 °C
Building component heat flux	
side 1	side 2
Max: 33.56 W/m²	Max: 4.85 W/m²
Min: -33.34 W/m²	Min: -4.64 W/m²
Range: 66.90 W/m²	Range: 9.49 W/m²

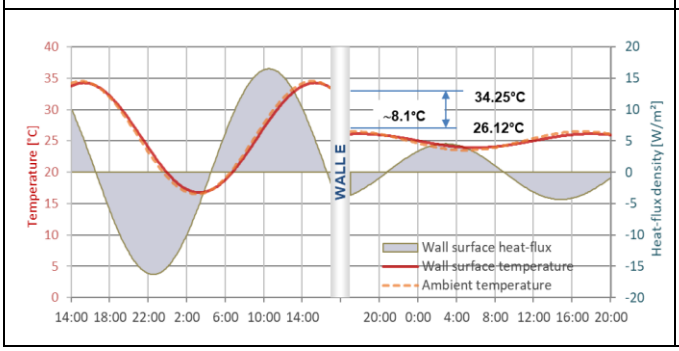

Building component surface temperature	
side 1	side 2
Max: 34.25 °C	Max: 26.12 °C
Min: -16.74 °C	Min: 23.90 °C
Range: 17.50 °C	Range: 2.21 °C
Building component heat flux	
side 1	side 2
Max: 16.49 W/m²	Max: 4.53 W/m²
Min: -16.32 W/m²	Min: -4.36 W/m²
Range: 32.81 W/m²	Range: 8.89 W/m²

Fig. 7 – Diurnal heat flow simulation for walls in July

Analysis of Figure 7 tabled data and a quantitative picture of heat-flaw and temperature behaviour leads to such intermediate takeaways:

- Despite significant differences in material composition, all wall types demonstrate a comparable internal thermal response. The interior surface temperature amplitudes remain within a narrow range (2.2 - 2.5 °C), while the internal heat flux amplitudes are similarly limited (4 - 5 W/m²). This indicates that all configurations provide an adequate level of indoor thermal stability under the considered climatic excitation.
- Substantial differences are observed at the external surface. The maximum external heat flux varies significantly between wall types (≈16–34 W/m²), indicating that the interaction between the building envelope and the outdoor environment is highly dependent on the wall structure.

The results confirm a clear functional separation of roles within multilayer assemblies:

- The external layer primarily governs the intensity of heat exchange with the environment, as reflected by the external heat flux amplitude ($q_{max,\ ext}$). This behaviour is strongly linked to the surface layer's thermal effusivity.
- The internal mass distribution controls the attenuation of the thermal wave, quantified by the decrement factor (f), and the heat storage capacity, expressed by (k_1).
- A low decrement factor does not necessarily imply a low external heat flux. In particular, the wood-chip concrete wall (Type D) exhibits one of the lowest decrement factors while simultaneously producing the highest external heat flux. This behaviour can be interpreted as a “high-intensity thermal accumulator”, which efficiently absorbs heat but interacts strongly with the external environment.
- In contrast, configurations incorporating external insulation (notably wall Type C) effectively decouple the external environment from the internal thermal mass. This leads to both reduced external heat flux and strong attenuation of the thermal wave. As a result, such assemblies achieve a more balanced performance.
- The hempcrete wall (Type A) demonstrates a well-balanced behaviour, combining moderate external heat flux with satisfactory attenuation and heat capacity. Conversely, the AAC-based wall (Type B) shows limited thermal inertia despite low external fluxes. In contrast, the ICF-type wall (Type E) minimises external heat exchange but utilises internal mass less effectively.
- The comparison between hempcrete and wood-chip cement-bonded concrete walls further highlights that, when boundary layers are identical, differences in performance are primarily driven by the internal core properties. In this case, variations in thermal effusivity of the core material have only a secondary influence on the external/internal flux ratio. At the same time, the decrement factor remains the dominant parameter governing internal heat flux.
- The study demonstrates that the dynamic thermal performance of building envelopes cannot be fully characterised by traditional parameters such as thermal transmittance or decrement factor alone. Instead, a multi-criteria perspective is required.
- An extended evaluation framework incorporating (k_1), (f), and (q_{max}) provides a more comprehensive basis for optimising multilayer wall assemblies than existing standards. This approach enables a more physically consistent interpretation of heat transfer processes and supports the development of energy-efficient and thermally stable building envelopes.

All the aforementioned evidence demonstrates that thermal inertia plays a crucial role in dynamic simulation and can be incorporated into multi-criteria optimisation and the pre-design assessment of building energy efficiency performance.

On the other hand, as stated in [40], in the case of countries with a hot summer climate, to which, as we evident, Ukraine can also be enlisted, in retrospect of harsh climate changes, especially in the recent few decades, the recommended range of dynamic thermal parameters, valid for energy efficient envelopes with $\mathrm{U-value} < 0.3 \frac{\mathrm{W}}{m^2\mathrm{K}}$ are $0.04 \leq f \leq 0.08$ for decrement factor and $k_1 \geq 40 \frac{kJ}{m^2\mathrm{K}}$ for internal area heat capacity. This is also correlated with revealed recommendations for designers – a range of high thermal inertia levels $k1 \geq 30 \frac{kJ}{m^2\mathrm{K}}$ for assemblies with no too low a decrement factor value $f \sim 0.07$ [8].

To determine which of the assemblies considered in current research meet the recommended ranges for both dynamic characteristics, a scatterplot in Figure 8 shows the dependence of internal area heat capacity (k_1) on the decrement factor (f) for five assemblies.

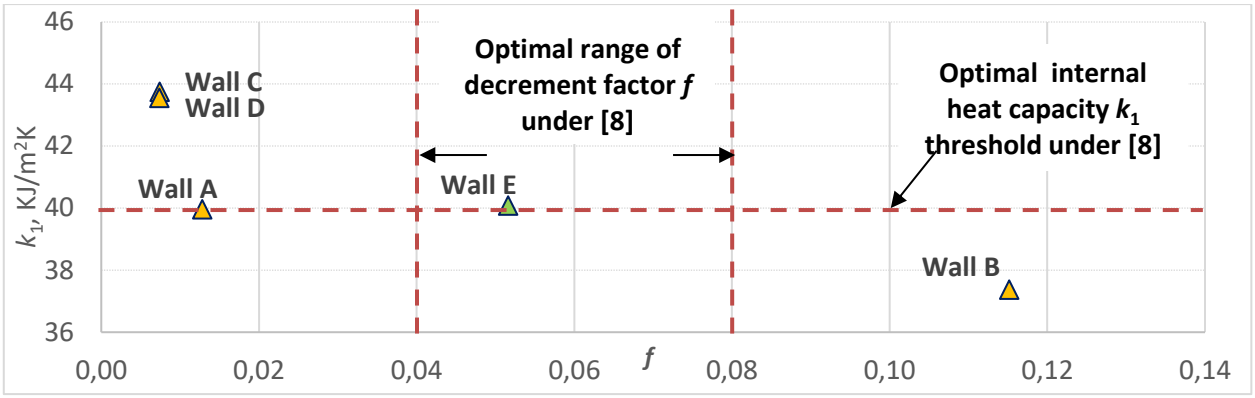

Fig. 8 – Factual arrangement of researched assemblies in terms of recommended (k_1) and (f) values

From Figure 8, it can be seen that only Wall E (marked in green) of all the researched types of assemblies falls within the recommended range of the (k_1) and (*f*) values. Wall B has the highest decrement factor (f) and the lowest (k_1) value, indicating that it has the lowest damping effect on the incoming heat flow, according to [2]. Walls A, C and D have a low decrement factor (*f*) with a good (k_1) value.

Thus, since this research involves more than one characteristic to compare (in the current study, there are five physical parameters), multicriteria decision analysis (MCDA) is applicable.

In this regard, new physically based criteria for energy efficiency assessment are proposed, which are aimed at eliminating the subjectivity of parameter weights, weighted sums, and other commonly used data manipulations that involve different units for calculating the goal function (e.g. weighted aggregation), aimed at interconnecting physical parameters to obtain global super criteria, which should be minimised or maximised.

For such a purpose, three criteria were proposed:

1) Dynamic thermal performance efficiency per mass m of the assembly, $DTPE_m$. This metric demonstrates how good the considered assembly is if we need to assess how much heat a material can store in terms of its mass, as shown in formula (14)

$$DTPE_m = \frac{k_1}{m} \tag{14}$$

2) Dynamic thermal performance efficiency per (*EE*) of the assembly, $DTPE_{EE}$, criteria which reflect how much thermal inertia of the assembly (k_1) is represented in terms of assembly (*EE*), as follows in formula (15)

$$DTPE_{EE} = \frac{k_1}{EE} \tag{15}$$

3) Dynamic thermal performance efficiency per mass (*m*) and (*EE*) of the assembly, $DTPE_{m\&EE}$, criteria which reflect how much thermal inertia of the assembly (k_1) is represented in terms of assembly mass (*m*) and (*EE*), as follows in formula (16)

$$DTPE_{m\&EE} = \frac{k_1}{EE \times m} \tag{16}$$

This formula provides a measure of how much heat a material can store relative to the energy required to produce it (*EE*) and its mass (*m*). It helps choose materials that are both energy-efficient and environmentally friendly - a higher value means the material is better at storing heat for less environmental cost (lower embodied energy); a lower value means the material requires more energy to produce for the amount of heat it stores, indicating lower thermal efficiency in terms of its environmental impact. As can be seen from the constituents of formulae (14)-(16), all the proposed criteria should be maximised.

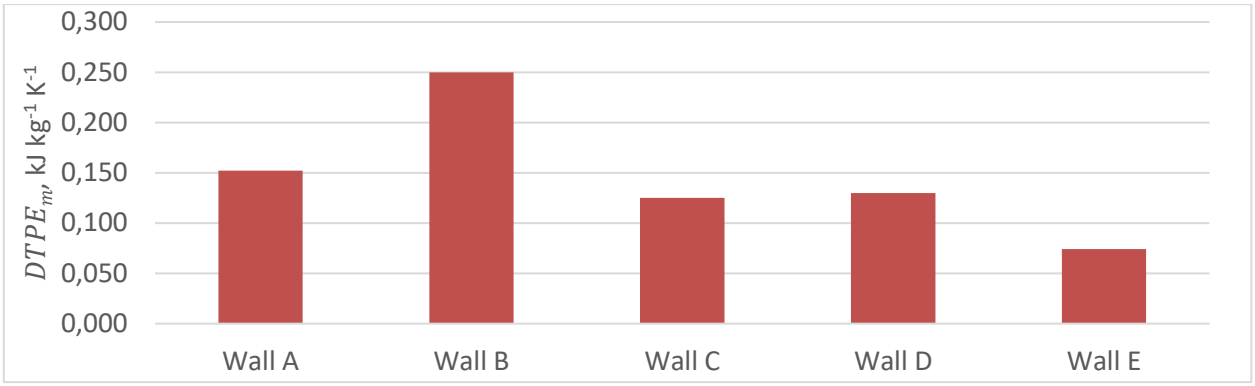

Fig. 9 – Dynamic thermal performance efficiency per mass m of the assembly $DTPE_m$, KJ/Kkg

From Figure 9, it can be seen that Wall B is the better alternative in terms of mass, as per the proposed criteria. Walls A, D and C have the same level of dynamic thermal performance. The Wall E can be considered the least preferable assembly in terms of the mass criteria. On the other hand, if we consider the EE criteria, the overall picture of the wall's preferences will change slightly (see Figure 10).

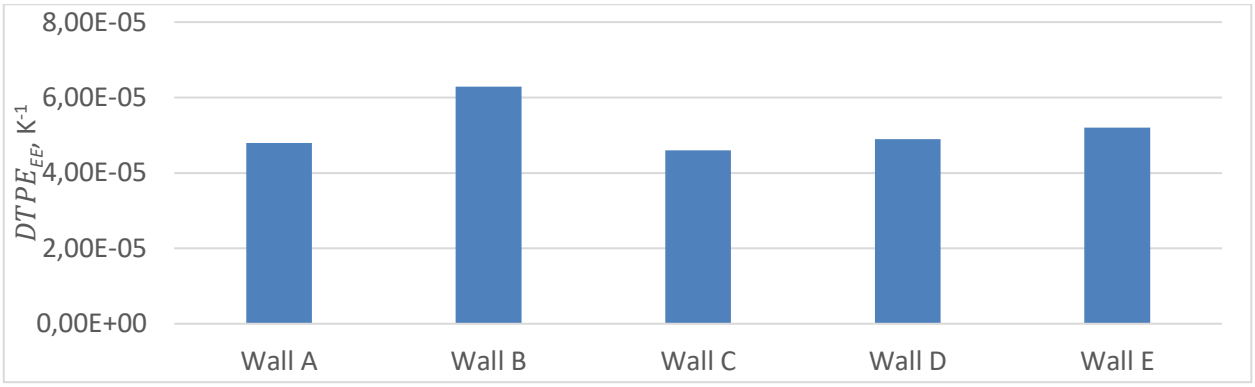

Fig. 10 – Dynamic thermal performance efficiency per embodied energy EE of the assembly $DTPE_{EE}$, 1/K

From Figure 10, it can be seen that Wall B remains the best alternative according to the proposed criteria; the remaining assemblies, namely Walls A, C, D, and E, exhibit approximately equal levels of (*EE*). Figure 11 illustrates the impact of both (*m*) and (*EE*) parameters on the proposed criteria.

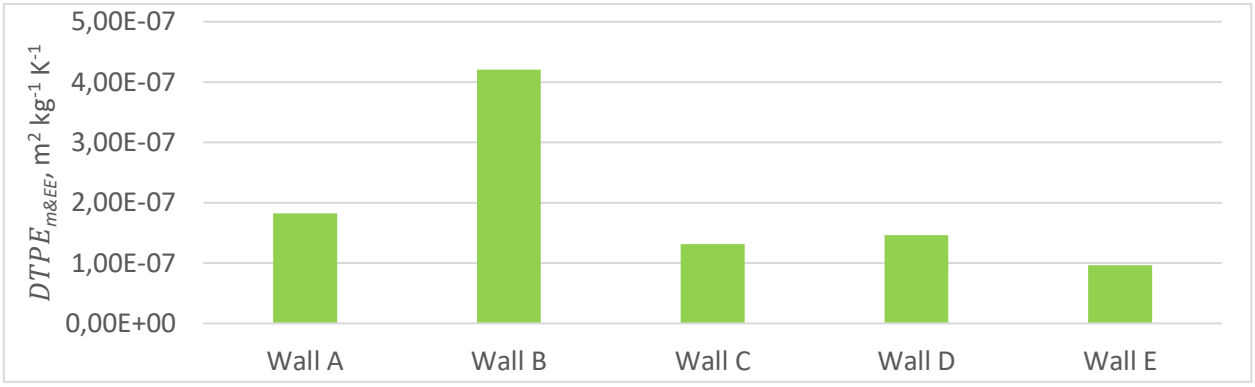

Fig. 11 - Dynamic thermal performance efficiency per mass m and embodied energy EE of the assembly $DTPE_{m\&EE}$, m^2/Kkg

From Figure 11, which illustrates how the value preferences change due to the product of the assembly mass (*m*) and embodied energy (*EE*), according to formula (16), been slightly changed with domination of Wall B as the best assembly and Wall E as the worst one, meanwhile, the relative values of the wall alternatives evaluations differences, given in Figure 9 and Figure 11, are non-evident. It can be concluded that the preference tendency of wall assemblies, reflected in Figure 9 (mass (*m*) parameter) and Figure 11 (mass (*m*) and embodied energy (*EE*) parameters), follows a similar pattern. This can be explained by minor differences in the (*EE*) parameter (Figure 10), which, when multiplied by (m), directly influence the values illustrated in Figure 11.

To perform a comparative analysis of the obtained results, illustrated in Figures 9 - 11, the ranking of the suggested criteria results, both with the factual criteria values, is aggregated in Table 5.

Tab. 5 - Factual arrangement of researched assemblies in terms of proposed criteria

Govern criteria		Wall A	Wall B	Wall C	Wall D	Wall E
Absolute value	$DTPE_m$, [kJ kg^{-1} K^{-1}]	0.152	0.250	0.125	0.130	0.074
	$DTPE_{EE}$, [K^{-1}]	4.79E-05	6.29E-05	4.60E-05	4.90E-05	5.20E-05
	$DTPE_{m\&EE}$, [m^2 kg^{-1} K^{-1}]	1.83E-07	4.21E-07	1.31E-07	1.46E-07	9.63E-08
Results ranking*	$DTPE_m$	4	1	5	3	2
	$DTPE_{EE}$	2	1	4	3	5
	$DTPE_{m\&EE}$	2	1	4	3	5

*1- the best, 5 - the worst.

From Table 5, it can be seen that Wall B is the best alternative according to all three of the proposed criteria. Wall D possess the third position. The rest of the assemblies, namely Wall A, C and E, have different ranks according to the proposed criteria, and their preference are arguable.

DISCUSSION OF THE RESULTS OF THE RESEARCH

The comparative analysis of the investigated multilayer wall assemblies reveals several fundamental aspects of their dynamic thermal behaviour under periodic boundary conditions:

Assessing the typical wall assemblies in terms of the proposed dynamic thermal performance inertia *DTPE* criteria has shown that Wall B is the “undisputable best” assembly, considering both mass *m* and embodied energy *EE* parameter with rank 1 (Excellent); Wall D possesses the medium position with rank 3 (Satisfactory); Wall A, C, and E have non-obvious and arguable preference order, thus they can have unexpectedly competitive options. Meanwhile, the $DTPE_{EE}$ preference order has the same pattern as well in $DTPE_{m\&EE}$ case considerations, with rank 2 (Good) for Wall A, rank 4 (Poor) for Wall C and rank 5 (Unsatisfactory) for Wall E. Dynamic thermal performance criteria $DTPE_m$ slightly differs from the evaluations of embodied energy $DTPE_{EE}$ and $DTPE_{m\&EE}$ considerations given above with rank 4 (Poor) for Wall A, rank 5 (Unsatisfactory) for Wall C and rank 2 (Good) for Wall E.

Notably, Wall E aligns with the recommendations of the (k_1) and f values ranges, and thermophysically, but in terms of embodied energy, it occupies the last position.

It should be noted that the proposed criteria do not aim to replace traditional optimisation methods but rather to complement them by providing physically interpretable indicators. The results demonstrate that different criteria can yield conflicting rankings, highlighting the inherently multi-objective nature of envelope design, even when based solely on the physical properties of envelope materials, while accounting for dynamic thermal characteristics and embodied energy as the LCA component.

CONCLUSION

Among the results of the research, the following can be considered the most valuable:

(1) Three new criteria for providing early-stage multilayered assembly design assessment of envelope energy-efficiency potential, based exclusively on physical parameters of envelope materials, by considering dynamic thermal characteristics (decrement factor (*f*), internal area heat capacity (k_1), kJ/m^{2}K as well as embodied energy (*EE*), MJ/m^2 as the LCA component, were proposed in current research.

(2) The thermal transmittance coefficient (U-value) can be considered only in the early stages of decision-making as the primary determinant of envelope efficiency; however, this parameter alone fails to accurately reflect the dynamic thermal behaviour of constructions and their inertia-related performance.

(3) Dynamic thermal performance parameters, such as, but not restricted to, decrement factor (*f*) and internal area heat capacity (k_1), are valuable parameters for effective assembly design in the early multilayered design stage, by utilising the recommended ranges of both for different climate zones, respectively, for energy-efficient envelopes with $\mathrm{U-value} < 0.3 \frac{\mathrm{W}}{m^2\mathrm{K}}$, such as $0.04 \leq f \leq 0.08$ and $k_1 \geq 40 \frac{kJ}{m^2\mathrm{K}}$ for internal area heat capacity for hot climates. In the current research, the Wall E (ICF block) is the only one that met the recommended range of (*f*) and (k_1) for the five assemblies used in the research.

(4) The easily calculable physical dynamic thermal performance efficiency criteria *DTPE* can be used as a predesign metric for both, based on inertia-related performance assembly performance, outlined in EN ISO 13786 [1]. Consideration of the embodied energy (*EE*) or primary energy of the wall component MJ/m^2, as the objective LCA marker [14], [15] was proposed.

(5) Benchmarking of considered assemblies in terms of dynamic thermal performance efficiency criteria based on assembly mass m ($DTPE_m$), assembly embodied energy (*EE*) ($DTPE_{EE}$), and both assembly mass (*m*) and (*EE*) ($DTPE_{m\&EE}$) revealed that:

a) Wall A and C have a non-obvious and arguable preference order based on the proposed criteria - rank 2 (Good) and rank 4(Poor) for Wall A, and rank 4(Poor) and rank 5 (Unsatisfactory) for Wall C, respectively;
b) Wall B is the “undisputable best” assembly, considering both mass (*m*) and the embodied energy (*EE*) parameter with rank 1 (Excellent). However, it is out of the recommended range of decrement factor (*f*) that is shown in limited thermal inertia despite low external fluxes;
c) Wall D possesses the medium position with rank 3 (Satisfactory);
d) Wall E meets the recommended range of decrement factor *f* and internal area heat capacity k_1, but has the rank 2 (Good) only from the term of $DTPE_m$ (mass (*m*) consideration). However, Wall-E shows the rank 5 (Unsatisfactory) in terms of assembly embodied energy (*EE*) ($DTPE_{EE}$) and both assembly mass (*m*) and (*EE*) ($DTPE_{m\&EE}$).

It is essential to highlight that the assembly's ranking will vary depending on the alternatives being compared. In one case, “the worst” can be the optimal given the available assemblies; in another, “the best” can be the unsatisfactory rank, and the results may be contradictory, requiring additional verification and analysis to confirm the “best” choice among the proposed alternatives.

Current research can be determined as the next step in the conceptual evaluation attitude, exclusively based on measurable physical parameters with emphasise on the dynamic thermal characteristics and embodied energy as the LCA component, which can provide a more objective comparison of different envelopes types in terms of their thermophysical and physical-mechanical parameters, by elimination of the subjectivity of any data manipulations, such as parameter weights, weighted sums, and other commonly used methodologies that involve normalising the different parameter’s units for calculating the goal function (e.g. weighted aggregation).

LIST OF SYMBOLS

c	Specific heat capacity [kJ kg^{-1} K^{-1}]
f	Decrement factor
k_1	Internal area heat capacity of assembly [kJ m^{-2} K^{-1}]
$q_{max,\ ext}$	External heat flow intensity, [W m^{-2}]
T	Oscillation period [h]
U-value	Thermal transmittance coefficient of assembly [W m^{-2} K^{-1}]
Z_{ee}	Thermal transmittance matrix of a multilayered assembly
Z_i	Thermal transmittance matrix of the i-th layer of assembly
Z_{s1}	Boundary layer thermal transmittance matrix (exterior)
Z_{s2}	Boundary layer thermal transmittance matrix (interior)
$z11_i$	Thermal transmittance matrix component of the i-th layer of assembly
$z12_i$	Thermal transmittance matrix component of the i-th layer of assembly [m^2 K W^{-1}]
$z21_i$	Thermal transmittance matrix component of the i-th layer of assembly [W m^{-2} K^{-1}]
$z22_i$	Thermal transmittance matrix component of the i-th layer of assembly

Abbreviations

$DTPE_m$	Dynamic thermal performance efficiency per mass of the assembly [kJ kg^{-1} K^{-1}]
$DTPE_{EE}$	Dynamic thermal performance efficiency per embodied energy of the assembly [K^{-1}]
$DTPE_{m\&EE}$	Dynamic thermal performance efficiency per mass and embodied energy of the assembly [m^2 kg^{-1} K^{-1}]
EE	Embodied energy of assembly [MJ m^{-2}]

Greek symbols

λ	Thermal conductivity coefficient [W m^{-1} K^{-1}]
δ	Heat flux penetration depth [m]
ρ	Density [kg m^{-3}]
ξ	Dimensionless heat flux penetration depth

REFERENCES

[1] Thakkar, J. J. (2021). Multi-criteria decision making (Vol. 336, pp. 1-365). Singapore: Springer. https://doi.org/10.1007/978-981-33-4745-8

[2] Basińska, M. (2017). The use of multi-criteria optimisation to choose solutions for energy-efficient buildings. Bulletin of the Polish Academy of Sciences. Technical Sciences, 65(6). https://doi.org/10.1515/bpasts-2017-0084

[3] Wang, J. J., Jing, Y. Y., Zhang, C. F., & Zhao, J. H. (2009). Review of multi-criteria decision analysis in aid of sustainable energy decision-making. Renewable and sustainable energy reviews, 13(9), 2263-2278. https://doi.org/10.1016/j.rser.2009.06.021

[4] Biks Y., Ratushnyak, G., & Ratushnyak, O. (2019). Energy performance assessment of envelopes from organic materials. Architecture, Civil Engineering, Environment, 12(3), 55-67. https://doi.org/10.21307/acee-2019-036

[5] Brojan, L., Petric, A., Clouston, P. L. (2013). A comparative study of brick and strawbale wall systems from environmental, economical and energy perspectives. ARPN Journal of Engineering and Applied Sciences, 8, 920–926.

[6] Ukrainian National Standard. DSTU EN ISO 13786:2023 Thermal performance of building components – Dynamic thermal characteristics – Calculation methods (2023). (Official edition) Kyiv: Institute of Technical Thermophysics of the National Academy of Sciences of Ukraine (in Ukrainian).

[7] Alkhatib, H., & Lemarchand, P. (2024). Assessing Thermal Performance: An Experimental Study on U-Value Variability in Building Fabric Elements. Results in Engineering. https://doi.org/10.1016/j.rineng.2024.103730

[8] Stazi, F. (2017). Thermal Inertia in Energy Efficient Building Envelopes. Butterworth-Heinemann. https://doi.org/10.1016/C2016-0-00641-1

[9] Humaish, H.H., Marmoret, L., & Beji, H. (2018). Effect of thermal inertia (time lag and decrement factor) on the insulation thermal capacity. 2018 International Conference on Advance of Sustainable Engineering and its Application (ICASEA), 137-141. https://doi.org/10.1109/icasea.2018.8370971

[10] Ferrari, S., & Zanotto, V. (2016). Approximating Dynamic Thermal Behaviour of the Building Envelope. https://doi.org/10.1007/978-3-319-24136-4_2

[11] Pérez, G., Allegro, V.R., Alonso, C., Martín-Consuegra, F., Oteiza, I., Frutos, B., & Guerrero, A. (2019). Selection of suitable materials for the development of an innovative thermochromic Trombe wall. Advances in Building Energy Research, 15, 146 - 160. https://doi.org/10.1080/17512549.2019.1684364

[12] Auf Hamada, A., Raslan, R., & Hong, S. (2023). A framework for parametric multi-criteria decision analysis (P-MCDA) for building retrofits. Building Simulation Conference Proceedings. https://doi.org/10.26868/25222708.2023.1519

[13] Kovalenko, I., Davydenko, Y., Shved, A. (2020). Searching for Pareto-Optimal Solutions. In: Shakhovska, N., Medykovskyy, M.O. (eds) Advances in Intelligent Systems and Computing IV. CSIT 2019. Advances in Intelligent Systems and Computing, vol 1080. Springer, Cham. https://doi.org/10.1007/978-3-030-33695-0_10

[14] Asdrubali, F., Grazieschi, G., Roncone, M., Thiébat, F., & Carbonaro, C. (2023). Sustainability of Building Materials: Embodied Energy and Embodied Carbon of Masonry. Energies. https://doi.org/10.3390/en16041846

[15] Reilly, A., Kinnane, O., & O'Hegarty, R. (2020). Energy embodied in, and transmitted through, walls of different types when accounting for the dynamic effects of thermal mass. Journal of Green Building, 15(4), 43-66. https://doi.org/10.3992/jgb.15.4.43

[16] Oktay, H., Argunhan, Z., Yumrutaş, R., Işık, M. Z., & Budak, N. (2016). An investigation of the influence of thermophysical properties of multilayer walls and roofs on the dynamic thermal characteristics. Mugla Journal of Science and Technology, 2(1), 48-54

[17] Verbeke, S., & Audenaert, A. (2018). Thermal inertia in buildings: A review of impacts across climate and building use. Renewable and sustainable energy reviews, 82, 2300-2318. https://doi.org/10.1016/j.rser.2017.08.083.

[18] Barbhuiya, S., & Das, B. B. (2023). Life Cycle Assessment of construction materials: Methodologies, applications and future directions for sustainable decision-making. Case Studies in Construction Materials, 19, e02326. https://doi.org/10.1016/j.cscm.2023.e02326.

[19] Young, L., Kaminski, S., Kovacs, M., & Zea Escamilla, E. (2024). A Comparative Life Cycle Assessment (LCA) of a Composite Bamboo Shear Wall System Developed for El Salvador. Sustainability, 16(17), 7602. https://doi.org/10.3390/su16177602

[20] Childs, K. W., Courville, G. E., & Bales, E. L. (1983). Thermal mass assessment: an explanation of the mechanisms by which building mass influences heating and cooling energy requirements (No. ORNL/CON-97). Oak Ridge National Lab.(ORNL), Oak Ridge, TN (United States). https://doi.org/10.2172/5788833

[21] Reilly, A., & Kinnane, O. (2017). The impact of thermal mass on building energy consumption. Applied Energy, 198, 108-121. https://doi.org/10.1016/j.apenergy.2017.04.024

[22] Eco2soft. Life cycle assessment of buildings. Retrieved June 28, 2025, from: https://www.baubook.at/eco2soft/?SW=27&LU=1823785713&qJ=1&LP=b4BKI&lng=2.

[23] A brief guide and free tool for the calculation of the thermal mass of building components. Retrieved February 18, 2026, from: https://www.htflux.com/en/free-calculation-tool-for-thermal-mass-of-building-components-iso-13786/

[24] Isotex. (n.d.). Isotex: Wood-cement blocks for construction. Retrieved June 5, 2025, from https://en.blocchiisotex.com/

[25] Isotex Srl. (2025) Product catalogue. Retrieved July 19, 2025 from https://www.blocchiisotex.com/wp-content/uploads/2025/02/product-catalogue-isotex-worldwide.pdf

[26] Fixolite. (2009). Brochure: Blocs de construction isolants en aggloméré bois-ciment. La performance au service de l'éco-construction [document PDF]. Retrieved June 22, 2025, from http://www.fixolite.be/sites/fixolite.be/files/Brochure_Blocs_Fixolite_ENTETE_VERTEmodif.pdf

[27] Isolabloc. (2025). Le futur se construit. Retrieved June 22, 2025, from http://www.isolabloc.fr

[28] Isospan. (2025). Technical Data and Product Range. Retrieved June 29, 2025, from https://www.isospan.eu/cms/upload/dlmstat/index.php?sprache=en

[29] Fasswall®. Build your natural, non-toxic home with this remarkable wood-chip concrete building block. Retrieved March 20, 2026, from https://faswall.com/
[30] Nexcem. Insulated Concrete Forms without Styrofoam. Retrieved March 20, 2026, from https://nexcembuild.com/
[31] Durisol. DURISOL ICF INSULATED CONCRETE FORMS FOR AUSTRALIA. Retrieved March 20, 2026, from https://www.durisol.com.au/
[32] Костробетон — революційна новинка на ринку екобудівництва (Hemcrete – a new revolutionary innovation on the ecobuilding maket) Retrieved March 20, 2026, from https://zelenasadyba.com.ua/dim-i-podvirya/kostrobeton.html (in Ukrainian)
[33] Утеплення будинку з газобетону зовні: як правильно це зробити? (House exterior insulation – how to perform it correctly?) Retrieved March 20, 2026, from http://gazobloki.lviv.ua/uteplennya-budinku-z-gazobetonu-zovni-yak-pravilno-ce-zrobiti/ (in Ukrainian)
[34] Porotherm 38 P+W. Retrieved March 20, 2026, from https://info-haus.com/product/porotherm-38-p-w/ (in Ukrainian)
[35] Будинок з арболіта — будівництво будинку своїми руками (House made of arbolit — DIY construction). Retrieved March 20, 2026, from https://stroyfibra.com.ua/budinok-z-arbolita-budivnictvo-budinku-svoimi-rukami/ (in Ukrainian)
[36] Building Better with ISOTEX. Retrieved March 20, 2026, Retrieved March 20, 2026, from https://murotex.co.uk/about-us/
[37] Ukrainian National Standard. DSTU N B V.2.6-101:2010. (2010). Constructions of buildings and structures. Method for determination of thermal resistance of building envelopes. Kyiv, Institute of Technical Thermophysics of the National Academy of Sciences of Ukraine (in Ukrainian).
[38] Filonenko, O. I., Yurin, O. I. (2015). (Construction and Thermal Physics of Building Enclosures: A manual (Poltava: Poltava National Technical University named after Yuri Kondratyuk), (in Ukrainian).
[39] Ukrainian National Standard. DSTU 9191:2022. (2022). Thermal insulation of buildings. Method for selecting thermal insulation material for building insulation. (Official edition). Kyiv: Ministry of Economy of Ukraine (in Ukrainian).
[40] Shea, A., Lawrence, M., & Walker, P. (2012). Hygrothermal performance of an experimental hemp-lime building. Construction and Building Materials, 36, 270–275. https://doi.org/10.1016/j.conbuildmat.2012.04.123
[41] Le, A. T., Maalouf, C., Mai, T. H., Wurtz, E., & Collet, F. (2010). Transient hygrothermal behaviour of a hemp concrete building envelope. Energy and buildings, 42(10), 1797-1806. https://doi.org/10.1016/j.enbuild.2010.05.016
[42] Evrard, A. (2008, May). Transient hygrothermal behaviour of lime-hemp materials (Doctoral thesis). Ecole Polytechnique de Louvain, Unité d'Architecture.
[43] Walker, R., & Pavia, S. (2014). Moisture transfer and thermal properties of hemp-lime concretes. Construction and Building Materials, 64, 270-276. https://doi.org/10.1016/j.conbuildmat.2014.04.081
[44] Florentin, Y., Pearlmutter, D., Givoni, B., & Gal, E. (2017). A life-cycle energy and carbon analysis of hemp-lime bio-composite building materials. Energy and Buildings, 156, 293-305. https://doi.org/10.1016/j.enbuild.2017.09.097
[45] Porotherm – Wall solutions. Retrieved July 20, 2025 from https://porotherm.com.ua/pdf/Porotherm_P_W_RU.pdf
[46] Porotherm Technical datasheet Porotherm BIO Inc. 38 T. Retrieved July 20, 2025, from https://www.infobuild.it/wp-content/uploads/Porotherm-BIO-inc-38-25-19-T.pdf
[47] Neopor® – a Raw Material for Diverse Solutions. Retrieved July 19, 2025 from https://neopor.de/portal/load/fid1225927/Neopor_Thermal_insulation.pdf
[48] Rockwool SIUPERROCK. Retrieved July 20, 2025, from https://www.rockwool.com/ua/products-and-applications/products/ua-diy/SUPERROCK-UA/
[49] Ukrainian National Building Code. Thermal insulation and energy efficiency of buildings: DBN V.2.6-31:2021 (2021). (Official edition). Kyiv: Ministry for Communities and Territories Development of Ukraine. (in Ukrainian).
[50] Stazi, F., Ulpiani, G., Pergolini, M., & Di Perna, C. (2018). The role of areal heat capacity and decrement factor in case of hyper insulated buildings: An experimental study. Energy and Buildings, 176, 310-324. https://doi.org/10.1016/j.enbuild.2018.07.034

[51] Shaik, S., & Setty, A. B. T. P. (2013). Analytical computation of admittance, decrement factor, time lag and surface factors for different exterior wall materials of the buildings in Dakshina Kannada district. In Proc. 22th Natl. 11th Int. ISHMT-ASME Heat Mass Transf. Conf.

[52] Kalinović, S. M., Djoković, J. M., Nikolić, R. R., & Hadzima, B. (2019). Calculation of the thermal dynamic performance of the residential buildings' walls. Quality Production Improvement-QPI, 1.

[53] Kottek, M., Grieser, J., Beck, C., Rudolf, B., & Rubel, F. (2006). World map of the Köppen-Geiger climate classification updated

[54] Ukrainian National Standard. Energy efficiency of buildings. Method for calculating energy consumption during heating, cooling, ventilation, lighting and hot water supply: DSTU 9190:2022 (2022). (Official edition). Kyiv: Ministry for Communities and Territories Development of Ukraine. (in Ukrainian).

[55] Ukrainian National Standard. Energy efficiency of buildings. Building climatology: DSTU N B V.1.1-27:2010 (2010). (Official edition). Kyiv: Minregionbud of Ukraine. (in Ukrainian).